RSC Advances

PAPER

View Article Online
View Journal | View Issue

Cite this: *RSC Adv.*, 2021, **11**, 36360

Controlling the adsorption of osteopontin for mediating cell behaviour by using self-assembled monolayers with varying surface chemistry†

Zhuoying Chen,‡[a] Yan Fan,‡[b] Lin Wang,[abd] Zhengqi Bian*[ac] and Lijing Hao*[aef]

Osteopontin (OPN) is an important protein for mediating cell behaviour on biomaterials. However, the interactions between the chemical groups on the biomaterial surface and OPN still need to be further clarified, which has restricted the application of OPN in biomaterial functionalization. In the present study, we developed different self-assembled monolayers (SAMs) with specific chemical groups, including SAMs-OH, SAMs-OEG, SAMs-COOH, SAMs-NH_2, and SAMs-PO_3H_2, to study the behavior of OPN on these SAMs. The results showed that SAMs-NH_2 could strongly adsorb OPN, and the amount of protein was highest on this material. Meanwhile, the lowest amount of OPN was present on SAMs-OEG. Interestingly, the unit-mass trend of bound OPN monoclonal antibodies (mAbs) on the SAMs was opposite to the OPN adsorption trend: lowest on SAMs-NH_2 but highest on SAMs-OEG. *In vitro* cell assay results showed that *mouse bone marrow mesenchymal stem cells* (*mBMSCs*) on SAMs-COOH, SAMs-NH_2, and SAMs-PO_3H_2 with pre-adsorbed OPN showed promoted behaviour, in terms of spreading, viability, and the expression levels of α_v and β_3 genes, compared with the other two SAMs, demonstrating the higher bioactivity of the adsorbed OPN. We believe that our findings will have great potential for developing OPN-activated biomaterials.

Received 25th May 2021
Accepted 22nd October 2021

DOI: 10.1039/d1ra04063d

rsc.li/rsc-advances

1. Introduction

The properties of biomaterials are mainly determined by the proteins adhering to their surfaces.[1,2] These proteins will regulate the cellular behaviors, *e.g.*, the cell adhesion and subsequent cell migration, proliferation, and differentiation.[3] Therefore, regulating the adhesion of proteins on the surface has become a significant strategy when developing novel biomaterials.[4] Recently, researchers have regulated the adhesion of proteins *via* controlling the topology[5] and composition[6] of the surface, or even through pre-immobilizing expected proteins or peptides.[7] Through these strategies, the performances of biomaterials can be improved significantly.

Among these strategies, surface chemistry can greatly influence protein adsorption and subsequent cellular behaviors.[8] To obtain general information, self-assembled monolayers (SAMs) on model substrates with single or mixed chemical groups have been developed[9]. By this method, researchers have explored the surface-related interactions between cells and proteins on different surfaces, *e.g.*, in studies involving fibronectin,[10] vitronectin,[11] laminin,[12] and collagen,[13] and demonstrated that various chemical groups on SAMs can direct the fates of cells.[14–17] These universal conclusions have greatly improved the performances of biomaterials.

However, it is still meaningful to further explore the relationships between surface chemical groups and other significant proteins. Among these proteins, osteopontin (OPN) is a member of the small integrin-binding ligand N-linked glycoprotein (SIBLING) family, and it is closely involved in the biological functions of several tissue types.[18] For example, OPN present in bone tissue can activate alkaline phosphatase to improve bone remodeling.[19–21] Therefore, it is worth clarifying OPN adsorption behavior and subsequent cell adhesion for the development of biomaterials.[22]

In this study, we evaluated OPN adsorption on SAMs with different chemical groups, *i.e.*, –OH, –OEG, –COOH, –NH_2, and –PO_3H_2 (Fig. 1a). Subsequently, we explored the correlation between OPN adsorption and the behavior of *mouse bone marrow mesenchymal stem cells* (*mBMSCs*). These findings will be of great significance for the rational design and development of OPN-activated biomaterials.

[a]*School of Materials Science and Engineering, South China University of Technology, Guangzhou 510640, China. E-mail: msbzq@scut.edu.cn*

[b]*National Engineering Research Center for Tissue Restoration and Reconstruction, Guangzhou 510006, China. E-mail: msljhao@scut.edu.cn*

[c]*Key Laboratory of Biomedical Engineering of Guangdong Province, Guangzhou 510006, China*

[d]*Key Laboratory of Biomedical Materials and Engineering of the Ministry of Education, Guangzhou 510006, China*

[e]*Innovation Center for Tissue Restoration and Reconstruction, Guangzhou 510006, China*

[f]*Bioland Laboratory (Guangzhou Regenerative Medicine and Health Guangdong Laboratory), 510005 Guangzhou, China*

† Electronic supplementary information (ESI) available. See DOI: 10.1039/d1ra04063d

‡ These authors contributed equally.

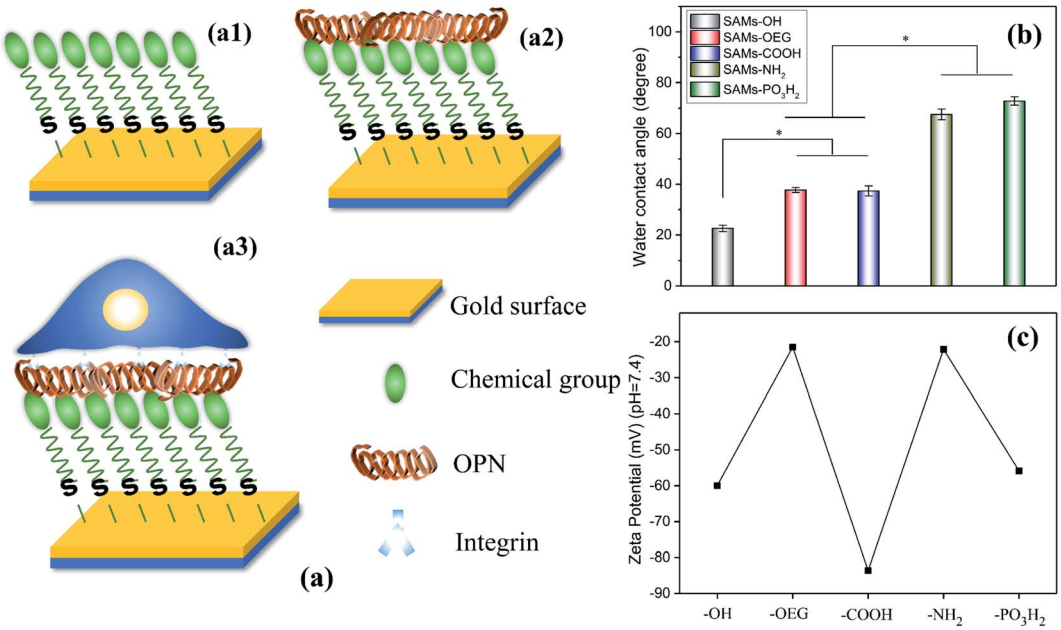

Fig. 1 (a) Preparing SAMs with different terminal chemical groups for OPN adsorption and cell adhesion studies: (a1) chemical groups (–OH, –OEG, –COOH, $-NH_2$, and $-PO_3H_2$) were first self-assembled on a gold slide; (a2) then OPN was adsorbed on the SAMs; and (a3) MSCs were finally seeded and adhered on these SAMs. (b) Surface wettability and (c) surface zeta potential data from the obtained SAMs. The stars in (b) indicate significant difference ($p < 0.05$).

2. Experimental

2.1 Preparation of SAMs

After being cleaned *via* nitrogen plasma treatment for 2 min, freshly cleaned gold slides (4 mm × 4 mm) were immediately immersed in either 11-mercapto-1-undecanol ($HS(CH_2)_{11}OH$, Dojindo, Japan), (11-mercaptoundecyl)hexa(ethylene glycol) ($HS(CH_2)_{11}(OCH_2CH_2)_6OH$, Dojindo, Japan), 10-carboxy-1-decanethiol ($HS(CH_2)_{10}COOH$, Dojindo, Japan), 11-amino-1-undecanethiol, hydrochloride ($HS(CH_2)_{11}NH_2HCl$, Dojindo, Japan), or 11-mercaptoundecylphosphoric acid ($HS(CH_2)_{11}$-OPO_3H_2, Sigma, USA) at 1 mmol L^{-1} and left overnight. Then, the substrates were rinsed alternately with ethanol and deionized water and dried under a stream of nitrogen gas. These samples are referred to as SAMs-OH, SAMs-OEG, SAMs-COOH, SAMs-NH_2, and SAMs-PO_3H_2.

2.2 Surface characterization

Static water contact angle measurements were performed using a contact angle meter (OCA15, Data Physics, Germany) ($n = 3$). The zeta potentials of surfaces were determined with an electrokinetic analyzer for solid surface analysis (SurPass, Anton Paar Austria) at a given pH value *via* pumping 10^{-3} mM KCl electrolyte ($n = 4$).

2.3 Protein adsorption

Recombinant mouse osteopontin (OPN) (R&D Systems, USA) was radiolabeled with ^{125}I, as described in another reference,[23] and then purified *via* size exclusion chromatography using Sephadex™ G-25 medium (GE Healthcare, Bio-Sciences AB, Sweden). SAM samples were immersed in protein solution (10 μg mL^{-1} in PBS) and incubated at 37 °C for 1 h. After rinsing with PBS, the radioactivity levels of samples were measured using a gamma radio-immunoassay counter (GC-300, USTC Chuangxin Co., Ltd, Zonkia Branch, China). Then the samples with adsorbed OPN were incubated in complete medium with 10% fetal bovine serum (FBS, Gibco, USA) at 37 °C for 1 h, rinsed, and measured again as previously described. The amount of adsorbed OPN on the surface (4 mm × 4 mm) was calculated from the radioactivity using the following equation ($n = 3$):

$$\text{Protein (ng cm}^{-2}) = \text{count (cpm)}/[A_{\text{solution}}\ (\text{cpm ng}^{-1}) \times S\ (\text{cm}^2)]$$

where count represents the radioactivity of the sample, and A_{solution} and S are the radioactivity of the protein solution and the surface area, respectively.

The exposure levels of cell-binding domains in adsorbed OPN were characterized *via* enzyme-linked immunosorbent assay (ELISA) studies with OPN monoclonal antibodies (OPN mAbs) (R&D Systems, USA) according to the manufacturer instructions ($n = 3$).

Besides OPN, we further characterized the adsorption of bovine serum albumin (BSA) (Sigma, USA) on the SAMs *via* surface plasmon resonance (SPR, Plexera® Bioscience LLC, USA) studies ($n = 5$). Briefly, SAMs were prepared on the SPR sensor (25 mm × 75 mm × 1 mm) surface *via* immersing the sensor in 12.5 mL of reaction solution (1 mM) for 24 h at room temperature, followed by washed by ethanol and deionized water. Then, each surface was treated with PBS, 50 μg mL^{-1} BSA, and PBS, successively, to remove weakly adsorbed proteins. An auto-injection system was used to control the sample flow at

a rate of 2 μL s^{-1}. The SPR sensorgram is expressed in refractive units (RU), where 1000 RU corresponds to a protein density of 1 ng mm^{-2}.

2.4 Cell adhesion and gene expression on SAMs

Mouse bone marrow mesenchymal stem cells (*mBMSCs*) (CRL-12424, ATCC, USA) from early passages (≤6) were collected for cell assays. The SAM substrates (10 mm × 10 mm) were immersed in 10 μg mL^{-1} OPN solution and incubated at 37 °C for 1 h. After rinsing with PBS, cells (5×10^4 cells per sample) were seeded on SAM samples with pre-adsorbed OPN and cultured in a serum-free medium. After 12 h of culturing, the cell cytoskeletal filamentous actin and nuclei were stained with Phalloidin FITC probe (AAT Bioquest® Inc., USA) for 20 min and DAPI (Beyotime, China) for 5 min, respectively. The cell morphologies were observed *via* confocal laser scanning microscopy (CLSM, Leica TCS SP5, Germany). Additionally, after 12 h of culturing, the viabilities of the adhered cells on SAMs was evaluated *via* Cell Counting Kit-8 (CCK-8, Dojindo, Japan) assays, immersing the samples into 300 μL of CCK-8 working solution for 1 h of incubation. The absorbance at 450 nm was measured with a microplate reader (Thermo3001, USA).

The gene expression levels of α_v and β_3 integrin in cells were tested *via* qRT-PCR assays. Briefly, after 12 h of culturing (5×10^4 cells per sample), the total RNA in the cells was isolated using HiPure Total RNA Kits (Magentec, China) and reverse-transcribed into cDNA using a PrimeScript® RT Reagent Kit with a gDNA Eraser (TaKaRa Biotechnology, Japan) according to the manufacturer protocol. RT-PCR reactions were conducted using an SYBR green system (Invitrogen, USA) as follows: heating at 95 °C for 10 min and then 40 cycles at 95 °C for 15 s and 60 °C for 1 min. The adopted primers (TaKaRa Biotechnology, Japan) are as follows – β-actin: forward: TTGCTCCGAACCACTGCAAG, reverse: GCTGGAAGGTGGACAGTGAG; α_v integrin: forward: TGAACTG-CACGGCAGATACAGAG, reverse: TAGCGCCGGAGTCTGTTCAC-TAC; β_3 integrin: forward: TTCAATGCCACCTGCCTCAA, reverse: CCTTGGCCTCGATACTAAAGCTCA.

2.5 Statistical analysis

Statistical comparisons were carried out *via* analysis of variance (ANOVA) followed by post-hoc tests. A p value < 0.05 was considered to be statistically significant.

3. Results and discussion

The chemical groups strongly affected the wettability and zeta potential of the SAMs. The contact-angle results showed that all the SAMs were hydrophilic (Fig. 1b). Specifically, SAMs-OH had the lowest contact angle of 22.6°, while SAMs-OEG and SAMs-COOH had contact angles of 37.7° and 37.3°, respectively. Meanwhile, the contact angles of SAMs-NH_2 and SAMs-PO_3H_2 increased to 67.5° and 72.8°, respectively. Additionally, the zeta potential results at pH 7.4 (Fig. 1c) showed that positively charged SAMs-OEG and SAMs-NH_2 had the highest zeta potentials of −21.49 mV and −22.09 mV and negatively charged SAMs-COOH had the lowest zeta potential of −83.63 mV. The zeta potentials of SAMs-OH and SAMs-PO_3H_2 were −59.95 mV and −55.82 mV, respectively. Some of the results had a similar trend to what was seen in our previous study,[17,24] demonstrating that SAMs exhibit distinct properties.

OPN adsorbed on the SAMs with significantly different adsorption behaviours. To quantify the amounts of OPN on the surfaces, we labelled the protein *via* ^{125}I radiolabeling, and the calculated iodination yield of ^{125}I-OPN was as high as 93.9% (Fig. 2a). The ^{125}I-OPN count results (Fig. 2b) showed that SAMs-NH_2 could strongly adsorb OPN; the adsorbed amount was 89.01 ± 13.62 ng cm^{-2}, which was 4.36-, 26.24-, 12.31- and 10.47-times the values of SAMs-OH, SAMs-OEG, SAMs-COOH and SAMs-PO_3H_2, respectively. This is likely to be caused by electrostatic forces between negatively charged OPN[25] and the positively charged surface. We also demonstrated that with an increase in pH from 5 to 9, the adsorbed amount of OPN increased on SAMs-NH_2, further verifying the presence of electrostatic forces, as an increase in the pH value will increase the negative charge of OPN (Fig. S1 and S2†). Notably, the adsorbed amounts of OPN on SAM-OEG, SAM-OH, SAM-COOH, and SAM-PO_3H_2 showed a negligible relationship to the pH value, demonstrating that electrostatic interactions were not dominant on these surfaces. Protein adsorption and interactions are governed by many factors, such as solution pH, ionic strength, the chemical nature of the salt, surface hydrophobicity, the surface charge distribution, and the protein phase behavior. Meanwhile, the amount of OPN on neutral SAMs-OH was 20.44 ± 4.73 ng cm^{-2}, which was higher than the amounts on negatively charged SAMs-COOH and SAMs-PO_3H_2 (7.23 ± 1.02 ng cm^{-2} and 8.50 ± 1.98 ng cm^{-2}, respectively). The amount of OPN was lowest on SAMs-OEG (3.39 ± 0.63 ng cm^{-2}) due to the non-fouling effects of OEG molecules.[26] Additionally, the retained amounts of adsorbed ^{125}I-OPN on SAMs after treatment with serum-containing medium were also measured (Fig. 2b). The results showed that serum proteins reduced the amounts of adsorbed OPN, as the Vroman effect meant that there was competitive adsorption between serum proteins and pre-adsorbed OPN.[27] However, treatment did not change the final adsorption trend, implying that adsorption between OPN and the SAMs was relatively stable.

Besides the adsorption amount, the chemical groups further affected the conformation of the proteins on SAMs. The ELISA results from bound OPN mAbs (Fig. 2c) showed that the exposure levels of cell-binding domains in adsorbed OPN were consistent with the adsorbed amounts of OPN. The amount of bound OPN mAbs on SAMs-NH_2 was highest, and it was 1.49-, 2.38-, 1.48-, and 1.32-times the amounts on SAMs-OH, SAMs-OEG, SAMs-COOH, and SAMs-PO_3H_2, respectively. Additionally, although there was more OPN on SAMs-OH than on SAMs-COOH and SAMs-PO_3H_2 (Fig. 2b), these three SAMs had comparable levels of bound OPN mAbs. Interestingly, the unit-mass trend of bound OPN mAbs on the SAMs was opposite to the OPN adsorption trend. Specifically, the unit mass of bound OPN mAbs on SAMs-NH_2 was lowest (Fig. 2d). One of the possible reasons was electrostatic forces between the surface and the protein, which could limit the flexibility of the adsorbed

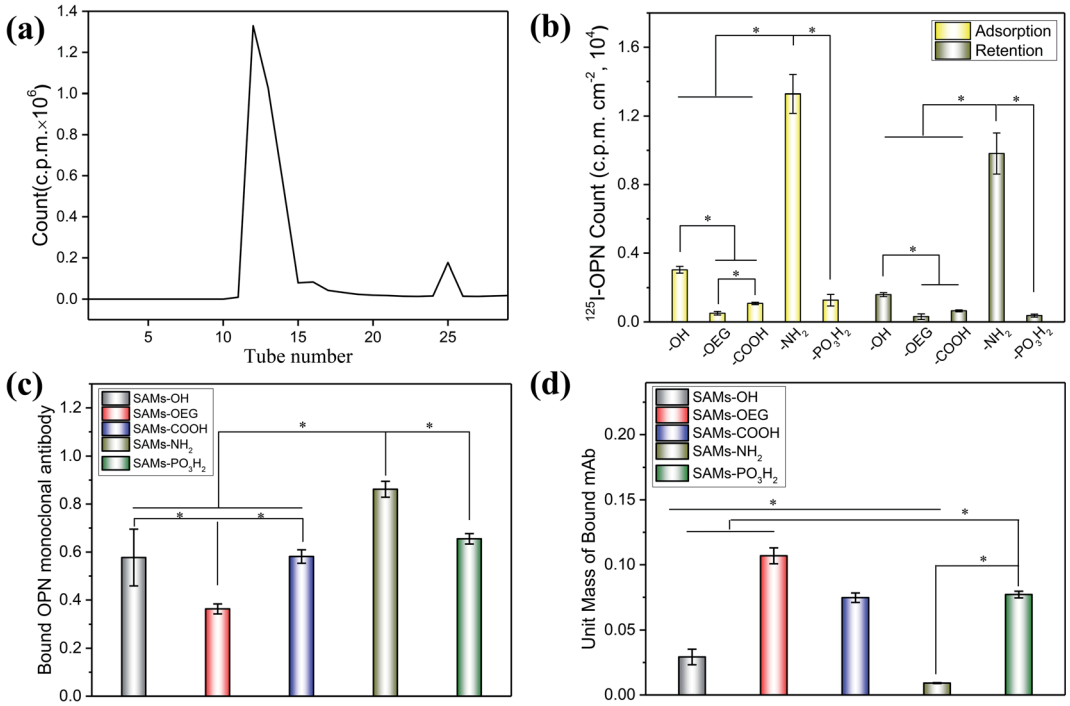

Fig. 2 The chromatographic fractionation curve of labeled ^{125}I-OPN obtained *via* the iodogen method (a), the initial adsorption and final retention amounts of ^{125}I-OPN on various SAMs (b), the binding domains of OPN on each SAM evaluated *via* ELISA (c), and the unit mass values of bound mAbs on the indicated surfaces (d). In (b), initial adsorption was calculated after rinsing with PBS, while final retention was obtained after further treatment with complete culture medium. The stars indicate significant difference ($p < 0.05$).

protein and decrease the exposure of bound OPN mAbs.[28] The unit mass of bound OPN mAb on SAMs-OEG was highest, as the weak interactions resulted in the high flexibility of the protein on the surface. Steric factors are another possible reason. The OPN molecules on SAMs would interact with other OPN molecules, and the higher density could significantly decrease the exposure of molecules.[29] Additionally, a difference in OPN attachment points on the SAMs could also impact the unit mass of bound OPN mAbs.[30]

We further characterized the adsorption behaviour of BSA on the SAMs (Fig. 3), as serum albumin is one of the most abundant plasma proteins.[31] The SPR results showed that BSA had similar adsorption behaviour to OPN, and there was much more BSA on SAMs-NH_2 than the other four SAMs. Additionally, BSA has less negative charge, is less phosphorylated, and has more hydrophobic pockets;[32] the amount of BSA absorbed on SAMs-NH_2 was higher than the amounts of OPN adsorbed on SAMs-PO_3H_2, SAMs-OH, SAMs-OEG, and SAMs-COOH. As expected, the minimum amount of adsorption was observed on SAMs-OEG.

As previously reported, cell adhesion is important for transmitting signals, and it can regulate subsequent cell behaviour.[33] Therefore, we employed *in vitro* cell assays to verify the bioactivity of OPN for cell adhesion. The morphologies of *mBMSCs* on SAMs with pre-adsorbed OPN (Fig. 4a) showed that the cells spread with obvious pseudopodia on SAMs-COOH, SAMs-NH_2, and SAMs-PO_3H_2. However, on SAMs-OH and SAMs-OEG, the cells exhibited poor behavior. The CCK-8 results (Fig. 4b) showed a similar trend; cells on SAMs-COOH, SAMs-NH_2, and SAMs-PO_3H_2 had higher viability than those on SAMs-OH (2.15-, 2.17-, and 2.21-fold higher, respectively) and SAMs-OEG (3.54-, 3.57-, and 3.64-fold higher, respectively). As reported, a high level of bound OPN mAbs indicates more binding domains for cells.[34] However, although the level of bound OPN mAbs on SAMs-NH_2 was highest, its cell viability was similar to those of SAMs-COOH and SAMs-PO_3H_2. This might be because bound OPN mAbs have a critical value for cell adhesion. Additionally, although the level of bound OPN mAbs on SAMs-OH was similar to those on SAMs-COOH and SAMs-PO_3H_2, its cell viability was much lower. This may be caused by the

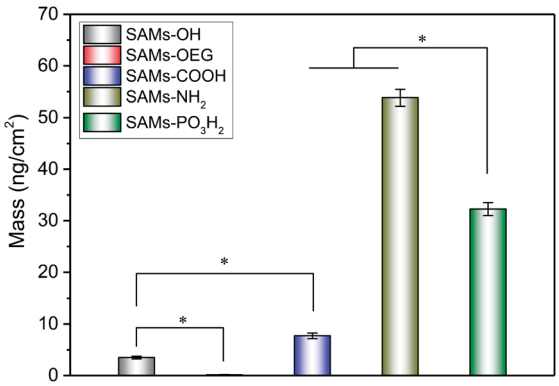

Fig. 3 The final masses of adsorbed protein on the SAM substrates from 50 μg mL^{-1} BSA solution.

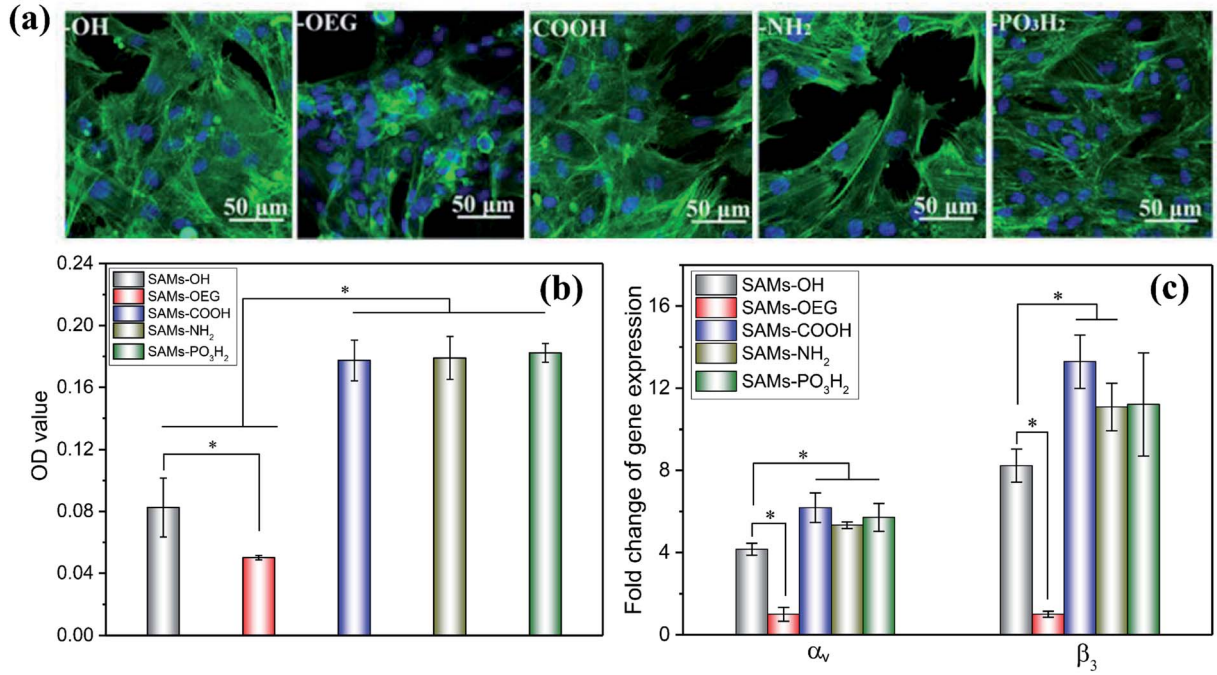

Fig. 4 The adhesion morphology observed *via* CLSM (a), the adhesion levels obtained *via* CCK-8 analysis (b), and the relative gene expression levels of α_v and β_3 obtained *via* q-PCR analysis (c) from the study of MSCs cultured on SAMs with pre-adsorbed OPN for 12 h. In (a), the green and blue fluorescence corresponds to F-actin and nuclei, respectively. The stars indicate significant difference ($p < 0.05$).

superhydrophilicity of the surface, which would impact the adhesion of cells due to the existence of a water membrane.[35]

Additionally, higher expression levels of α_v and β_3 by cells on SAMs-COOH, SAMs-NH_2, and SAMs-PO_3H_2 were observed. Specifically, the α_v gene expression levels on these three surfaces were 1.49-, 1.28-, 1.37-times higher, respectively, than on SAMs-OH, and 6.18-, 5.33-, and 5.71-times higher, respectively, than on SAMs-OEG. The β_3 gene expression levels on these three surfaces were 1.61-, 1.35-, and 1.36-times higher, respectively, than on SAMs-OH, and 13.29-, 11.08-, and 11.21-times higher, respectively, than on SAMs-OEG. As has been reported, primary interactions between cells and underlying proteins occur *via* integrins.[36] The upregulation of integrins was observed when their preferred ligands were available.[37] OPN has RGD adhesion motifs that are particularly likely to bind with integrins like $\alpha_v\beta_3$, $\alpha_v\beta_5$, and so on,[38] and it has been suggested that the expression of integrin subunit α_v and β_3 binding adhesion protein ligands can influence cell adhesion and subsequent activity[39]. Therefore, the different expression levels of α_v and β_3 by the cells on SAMs demonstrated that different chemical groups influenced cell adhesion through integrin-OPN binding.

Above all, we demonstrated that different chemical groups on SAMs affect the adsorption and conformation of OPN, further leading to different cell behaviours.

4. Conclusions

We demonstrated that the chemical groups on SAMs strongly affected the behavior toward OPN and the performance of OPN. The amount of adsorbed OPN was highest on SAMs-NH_2 (89.01 ± 13.62 ng cm^{-2}) and lowest on SAMs-OEG (3.39 ± 0.63 ng cm^{-2}). Interestingly, the unit-mass trend of bound OPN mAbs on SAMs was opposite to the OPN adsorption trend, which was because stronger interactions resulted in lower flexibility being shown by the adsorbed proteins. Meanwhile, cells on SAMs-COOH, SAMs-NH_2, and SAMs-PO_3H_2 with pre-adsorbed OPN showed larger spreading, better viabilities, and higher expression levels of α_v/β_3 genes than those on SAMs-OH and SAMs-OEG, demonstrating that OPN on these three SAMs exhibited higher bioactivity. Considering the significant effects of OPN on the biological functions of several tissue types, we believe that our research will provide great guidance for developing OPN-activated biomaterials.

Conflicts of interest

There are no conflicts of interest to declare.

Acknowledgements

This work was supported by the National Key R&D Program of China (2018YFA0703100, 2018YFC1105402, 2017YFC1104402, 2020YFB0204803), National Natural Science Foundation of China (31900959, 31700823, U1801252, 31771027), Natural Science Foundation of Guangdong Province of China (2020A1515011354), the Fundamental Research Funds for the Central Universities (2019MS003), the Guangdong Natural Science Funds for Distinguished Young Scholars (2019B151502029), the Outstanding Scholar Program of

Guangzhou Regenerative Medicine and Health Guangdong Laboratory (2018GZR110102001), and Key-Area Research and Development Program of Guangdong Province (2019B010940001). L. W. extends thanks to the Funds for Young Pearl River Scholars.

References

1 K. L. Christman, Biomaterials for tissue repair, *Science*, 2019, **363**, 340–341.
2 T. Hoshiba, C. Yoshikawa and K. Sakakibara, Characterization of Initial Cell Adhesion on Charged Polymer Substrates in Serum-Containing and Serum-Free Media, *Langmuir*, 2018, **34**, 4043–4051.
3 A. A. Khalili and M. R. Ahmad, A Review of Cell Adhesion Studies for Biomedical and Biological Applications, *Int. J. Mol. Sci.*, 2015, **16**, 18149–18184.
4 B. Trappmann, J. E. Gautrot, J. T. Connelly, D. G. T. Strange, Y. Li, M. L. Oyen, M. A. C. Stuart, H. Boehm, B. J. Li, V. Vogel, J. P. Spatz, F. M. Watt and W. T. S. Huck, Extracellular-matrix tethering regulates stem-cell fate, *Nat. Mater.*, 2012, **11**, 642–649.
5 M. S. Lord, M. Foss and F. Besenbacher, Influence of nanoscale surface topography on protein adsorption and cellular response, *Nano Today*, 2010, **5**, 66–78.
6 X. J. Liu, S. J. Shi, Q. L. Feng, A. Bachhuka, W. He, Q. L. Huang, R. R. Zhang, X. Yang and K. Vasilev, Surface Chemical Gradient Affects the Differentiation of Human Adipose-Derived Stem Cells *via* ERK1/2 Signaling Pathway, *ACS Appl. Mater. Interfaces*, 2015, **7**, 18473–18482.
7 R. Changede, H. Cai, S. J. Wind and M. P. Sheetz, Integrin nanoclusters can bridge thin matrix fibres to form cell-matrix adhesions, *Nat. Mater.*, 2019, **18**, 1366–1375.
8 M. Mrksich, What can surface chemistry do for cell biology?, *Curr. Opin. Chem. Biol.*, 2002, **6**, 794–797.
9 G. A. Hudalla and W. L. Murphy, Chemically well-defined self-assembled monolayers for cell culture: toward mimicking the natural ECM, *Soft Matter*, 2011, **7**, 9561–9571.
10 L. Parisi, A. Toffoli, B. Ghezzi, B. Mozzoni, S. Lumetti and G. M. Macaluso, A glance on the role of fibronectin in controlling cell response at biomaterial interface, *Jpn Dent. Sci. Rev.*, 2020, **56**, 50–55.
11 T. J. Li, L. J. Hao, J. Y. Li, C. Du and Y. J. Wang, Insight into vitronectin structural evolution on material surface chemistries: The mediation for cell adhesion, *Bioact. Mater.*, 2020, **5**, 1044–1052.
12 T. Miyazaki, S. Futaki, H. Suemori, Y. Taniguchi, M. Yamada, M. Kawasaki, M. Hayashi, H. Kumagai, N. Nakatsuji, K. Sekiguchi and E. Kawase, Laminin E8 fragments support efficient adhesion and expansion of dissociated human pluripotent stem cells, *Nat. Commun.*, 2012, **3**, 10.
13 J. Li, X. Mou, J. Qiu, S. Wang, D. Wang, D. Sun, W. Guo, D. Li, A. Kumar, X. Yang, A. Li and H. Liu, Surface Charge Regulation of Osteogenic Differentiation of Mesenchymal Stem Cell on Polarized Ferroelectric Crystal Substrate, *Adv. Healthcare Mater.*, 2015, **4**, 998–1003.
14 B. Cao, Y. Peng, X. Liu and J. Ding, Effects of Functional Groups of Materials on Nonspecific Adhesion and Chondrogenic Induction of Mesenchymal Stem Cells on Free and Micropatterned Surfaces, *ACS Appl. Mater. Interfaces*, 2017, **9**, 23574–23585.
15 M. A. Lan, C. A. Gersbach, K. E. Michael, B. G. Keselowsky and A. J. Garcia, Myoblast proliferation and differentiation on fibronectin-coated self assembled monolayers presenting different surface chemistries, *Biomaterials*, 2005, **26**, 4523–4531.
16 Y. Arima and H. Iwata, Effect of wettability and surface functional groups on protein adsorption and cell adhesion using well-defined mixed self-assembled monolayers, *Biomaterials*, 2007, **28**, 3074–3082.
17 L. J. Hao, T. J. Li, F. Yang, N. R. Zhao, F. Z. Cui, X. T. Shi, C. Du and Y. J. Wang, The correlation between osteopontin adsorption and cell adhesion to mixed self-assembled monolayers of varying charges and wettability, *Biomater. Sci.*, 2017, **5**, 800–807.
18 Q. Chen, P. Shou, L. Zhang, C. Xu, C. Zheng, Y. Han, W. Li, Y. Huang, X. Zhang, C. Shao, A. I. Roberts, A. B. Rabson, G. Ren, Y. Zhang, Y. Wang, D. T. Denhardt and Y. Shi, An Osteopontin-Integrin Interaction Plays a Critical Role in Directing Adipogenesis and Osteogenesis by Mesenchymal Stem Cells, *Stem Cells*, 2014, **32**, 327–337.
19 J. Sodek, B. Ganss and M. D. McKee, Osteopontin, *Crit. Rev. Oral Biol. Med.*, 2000, **11**, 279–303.
20 D. T. Denhardt and X. Guo, Osteopontin: a protein with diverse functions, *FASEB J.*, 1993, **7**, 1475–1482.
21 J. Maciel, M. I. Oliveira, R. M. Goncalves and M. A. Barbosa, The effect of adsorbed fibronectin and osteopontin on macrophage adhesion and morphology on hydrophilic and hydrophobic model surfaces, *Acta Biomater.*, 2012, **8**, 3669–3677.
22 L. Y. Liu, S. F. Chen, C. M. Giachelli, B. D. Ratner and S. Y. Jiang, Controlling osteopontin orientation on surfaces to modulate endothelial cell adhesion, *J. Biomed. Mater. Res., Part A*, 2005, **74**, 23–31.
23 S. N. Rodrigues, I. C. Goncalves, M. C. L. Martins, M. A. Barbosa and B. D. Ratner, Fibrinogen adsorption, platelet adhesion and activation on mixed hydroxyl-/methyl-terminated self-assembled monolayers, *Biomaterials*, 2006, **27**, 5357–5367.
24 L. Hao, H. Yang, C. Du, X. Fu, N. Zhao, S. Xu, F. Cui, C. Mao and Y. Wang, Directing the fate of human and mouse mesenchymal stem cells by hydroxyl-methyl mixed self-assembled monolayers with varying wettability, *J. Mater. Chem. B*, 2014, **2**, 4794–4801.
25 L. W. Fisher, D. A. Torchia, B. Fohr, M. F. Young and N. S. Fedarko, Flexible structures of SIBLING proteins, bone sialoprotein, and osteopontin, *Biochem. Biophys. Res. Commun.*, 2001, **280**, 460–465.
26 H. W. Ma, J. H. Hyun, P. Stiller and A. Chilkoti, "Non-fouling" oligo(ethylene glycol)-functionalized polymer brushes synthesized by surface-initiated atom transfer radical polymerization, *Adv. Mater.*, 2004, **16**, 338–341.

27 D. D. Stoebener, F. Paulus, A. Welle, C. Woell and R. Haag, Dynamic Protein Adsorption onto Dendritic Polyglycerol Sulfate Self-Assembled Monolayers, *Langmuir*, 2018, **34**, 10302–10308.

28 R. Jaenicke, Protein stability and molecular adaptation to extreme conditions, *Eur. J. Biochem.*, 1991, **202**, 715–728.

29 J. Maciel, M. I. Oliveira, R. M. Goncalves and M. A. Barbosa, The effect of adsorbed fibronectin and osteopontin on macrophage adhesion and morphology on hydrophilic and hydrophobic model surfaces, *Acta Biomater.*, 2012, **8**, 3669–3677.

30 C. C. Barrias, M. C. L. Martins, G. Almeida-Porada, M. A. Barbosa and P. L. Granja, The correlation between the adsorption of adhesive proteins and cell behaviour on hydroxyl-methyl mixed self-assembled monolayers, *Biomaterials*, 2009, **30**, 307–316.

31 D. C. Carter and J. X. Ho, Structure of serum albumin, *Adv. Protein Chem.*, 1994, **45**, 153–203.

32 V. Silin, H. Weetall and D. J. Vanderah, SPR studies of the nonspecific adsorption kinetics of human IgG and BSA on gold surfaces modified by self-assembled monolayers (SAMs), *J. Colloid Interface Sci.*, 1997, **185**, 94–103.

33 P. Roach, D. Farrar and C. C. Perry, Interpretation of protein adsorption: Surface-induced conformational changes, *J. Am. Chem. Soc.*, 2005, **127**, 8168–8173.

34 L. M. Weiner, R. Surana and S. Wang, Monoclonal antibodies: versatile platforms for cancer immunotherapy, *Nat. Rev. Immunol.*, 2010, **10**, 317–327.

35 C. P. Stallard, K. A. McDonnell, O. D. Onayemi, J. P. O'Gara and D. P. Dowling, Evaluation of Protein Adsorption on Atmospheric Plasma Deposited Coatings Exhibiting Superhydrophilic to Superhydrophobic Properties, *Biointerphases*, 2012, **7**, 31.

36 M. C. Siebers, P. J. ter Brugge, X. F. Walboomers and J. A. Jansen, Integrins as linker proteins between osteoblasts and bone replacing materials. A critical review, *Biomaterials*, 2005, **26**, 137–146.

37 D. Docheva, C. Popov, W. Mutschler and M. Schieker, Human mesenchymal stem cells in contact with their environment: surface characteristics and the integrin system, *J. Cell. Mol. Med.*, 2007, **11**, 21–38.

38 Y. Yokosaki, N. Matsuura, T. Sasaki, I. Murakami, H. Schneider, S. Higashiyama, Y. Saitoh, M. Yamakido, Y. Taooka and D. Sheppard, The integrin alpha(9)beta(1) binds to a novel recognition sequence (SVVYGLR) in the thrombin-cleaved amino-terminal fragment of osteopontin, *J. Biol. Chem.*, 1999, **274**, 36328–36334.

39 M. K. Majumdar, M. Keane-Moore, D. Buyaner, W. B. Hardy, M. A. Moorman, K. R. McIntosh and J. D. Mosca, Characterization and functionality of cell surface molecules on human mesenchymal stem cells, *J. Biomed. Sci.*, 2003, **10**, 228–241.